Random sequential adsorption of partially ordered discorectangles onto a continuous plane

Nikolai I. Lebovka [1,2,*] Nikolai V. Vygornitskii [1] and Yuri Yu. Tarasevich [3,†]

[1]*Department of Physical Chemistry of Disperse Minerals, F. D. Ovcharenko Institute of Biocolloidal Chemistry,*
NAS of Ukraine, Kyiv 03142, Ukraine
[2]*Department of Physics, Taras Shevchenko Kyiv National University, Kyiv 01033, Ukraine*
[3]*Laboratory of Mathematical Modeling, Astrakhan State University, Astrakhan 414056, Russia*

A computer simulation was used to study the random sequential adsorption of identical discorectangles onto a continuous plane. The problem was analyzed for a wide range of discorectangle aspect ratios ($\varepsilon \in [1; 100]$). We studied the anisotropic deposition, i.e., the orientations of the deposited particles were uniformly distributed within some interval such that the particles were preferentially aligned along a given direction. The kinetics of the changes in the packing fraction found at different values of such the alignment are discussed. Partial ordering of the discorectangles significantly affected the packing fraction at the jamming state, φ_j, and shifted the cusps in the $\varphi_j(\varepsilon)$ dependencies. The structure of the jammed state was analyzed using the adsorption of disks of different diameters into the porous space between the deposited discorectangles. The analysis of the connectivity between the discorectangles was performed assuming a core-shell structure of particles.

I. INTRODUCTION

The behavior of systems of interacting elongated particles continues to attract great attention in both academic and applied fields. In such systems, complex collective behavior, spontaneous orientational ordering, and self-assembly have been observed [1–3]. In particular, systems of elongated particles have shown a nematic orientational ordering in both thermal equilibrium [4,5] and athermal ($T = 0$) systems (for example, uniform shear flow [6]). The self-assembly of particles achieving their densest packing [7], and the crystallization transition (granular crystallization) from random to ordered packings under mechanical vibration have been observed [8]. The particle shape may affect not only the packing characteristics of powders and granular materials, and of porous media (e.g., packing fraction and coordination numbers) [9–11], but also the processes of aggregation [12], gravity- and vibration-induced segregation [13], compression behavior [14], and fluid flow through the porous packings [15]. A proper description of these processes is of fundamental importance for the preparation of advanced nanomaterials [16,17], specifically those filled by nanotubes [18] and nanoplatelets [19]. The structure of packings filled by elongated particles can significantly affect the connectivity, electrical conductivity, and permeation of such porous networks [20].

In recent decades, the many important practical applications of thin films [21,22] have initiated great interest in studies of two-dimensional (2D) systems filled with elongated particles [23]. The rich phase behavior in these systems has been observed in its dependence on the confining dimension [24]. Monte Carlo (MC) simulations of 2D systems of infinitely thin hard rods in thermal equilibrium have revealed a "nematic" phase at high densities [25]. However, such a "nematic" phase possessed algebraic order (quasi-long-range order). For 2D fluids of discorectangles (rounded-cap rectangles) [26], simulations have revealed that the "nematic" phase can be observed only for sufficiently long particles with aspect ratios (ε, length-to-width ratio) above 7. Shorter particles do not exhibit a "nematic" phase but undergo a melting transition.

Packing problems for nonequilibrium 2D systems of elongated particles have been intensively studied using a random sequential adsorption (RSA) model [27,28]. In this model, the particles are deposited randomly and sequentially onto a substrate, while overlapping with previously placed particles is strictly forbidden. For the RSA model, above some limiting coverage φ_j (called the jamming or saturation limit), there is no empty space for the deposition of a new particle and the adsorption process terminates.

The RSA simulations for disks gave a jamming coverage $\varphi_j = 0.547 \pm 0.002$ [29,30]. 2D saturated RSA packings of unoriented ellipses [31], squares [32], rectangles [33,34], discorectangles [35,36], polygons [37,38], sphere dimers, sphere polymers, and other shapes [39–41] have been investigated. For all the studied problems, cusplike maximums of jamming coverage at some aspect ratios ($\varepsilon \approx 1.7$–1.9) were observed. For very elongated shapes ($\varepsilon \gg 1$), the value of φ_j descended to zero according to the power law [42]:

$$\varphi_j \propto \varepsilon^{-1/(1+\sqrt{2})}. \tag{1}$$

For discorectangles, the observed maximum in jamming coverage was explained by the peculiar nearest-neighbor

*Corresponding author: lebovka@gmail.com
†Corresponding author: tarasevich@asu.edu.ru

relative orientation for short particles [35]. Similar cusplike maximums in the $\varphi_j(\varepsilon)$ dependencies have also been observed for saturated RSA packings of elongated particles in one-dimensional (1D) [43–46] and three-dimensional (3D) [3,23] systems. The kinetics of packing growth has been also studied in detail [30,31,33,34,41,42,47]. In particular, it was demonstrated that the asymptotic kinetics of the RSA of nonspherical particles is not the same as for spherical ones [47].

However, almost all previous studies of the saturated packing of elongated particles have been devoted to conventional RSA with unoriented particles. In some works, the RSA problems for perfectly oriented particles with respect to a selected direction; for example, parallel squares [48] and ideally oriented superdisks [49] have been studied. Recently the thermal relaxation towards equilibrium of 2D oriented RSA packings have been investigated [50]. Here the rods were infinitely thin ($\varepsilon = \infty$), and in the initial state, before relaxation, they were preferentially aligned with respect to a selected direction. The study revealed different relaxation behavior dependent on the preliminary ordering and the number density of the rods.

Experimental studies have reported various effects of the alignment of elongated particles on the transport and optical properties of thin films [51,52]. Various alignment techniques have been proposed to organize elongated particles onto 2D substrates, based on external forces (magnetic [53], electrical [54,55]), and shear flow [52]. This paper analyzes the RSA packing of identical elongated particles (discorectangles) on a 2D surface. We employ an off-lattice model, i.e., both the positions and orientations of the particles are continuous. The deposited particles were preferentially aligned along a selected direction. The aspect ratio of the particles varied within the range $\varepsilon \in [1; 100]$. Special attention has been paid to the effects of the alignment of the particles on the packing characteristics.

The rest of the paper is constructed as follows. In Sec. II the technical details of the simulations are described, all necessary quantities are defined, and some test results are presented. Section III describes our principal findings. Section IV summarizes the main results.

II. COMPUTATIONAL MODEL

A discorectangle is a rectangle with two hemidisks at its ends. The aspect ratio is defined as $\varepsilon = l/d$, where l is the total length of the particle and d is its width. The 2D packings were produced using an RSA model [27]. The particles were randomly and sequentially deposited onto a 2D surface until they reached the maximum (jamming) coverage φ_j. The overlapping of any new particle with previously deposited ones was forbidden (Fig. 1). For detecting overlapping during the deposition a fast algorithm to evaluate the shortest distance between particles was used [56–58]. The optimized RSA algorithm based on tracking of local regions was used [36]. Periodic boundary conditions were applied to the substrate in both the x and y directions.

The preferential orientation of the particles was characterized using the order parameter defined as
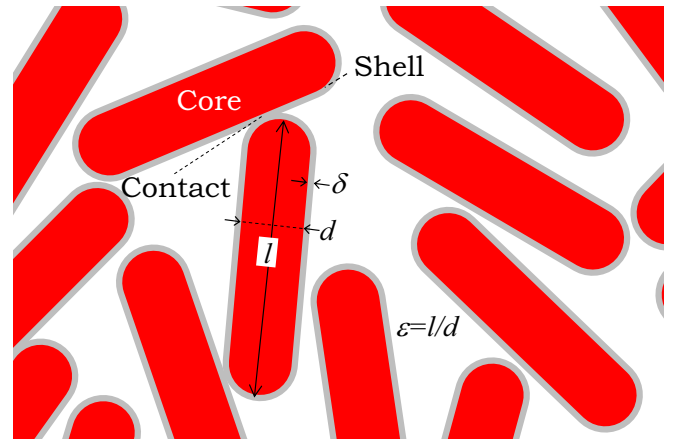
$$S = \langle \cos 2\theta \rangle, \qquad (2)$$

FIG. 1. An illustration of the RSA model of the packing of discorectangles on a 2D substrate. Intersections of the particle cores are forbidden. For the connectivity analysis, each particle is assumed to be covered by a soft (penetrable) shell with thickness δ.

where $\langle \cdot \rangle$ denotes the average, θ is the angle between the long axis of the particle and the selected direction, and x (the horizontal axis). For completely aligned and unoriented particles $S = 1$, and $S = 0$, respectively.

For producing partially ordered RSA deposits, a model of anisotropic random-orientation distribution has been used [59]. For this model, the orientations of the deposited particles are selected to be uniformly distributed within some interval $\theta \in [-\theta_m; \theta_m]$, where $\theta_m \leqslant \pi/2$. In this case, the preassigned order parameter can be evaluated as [50]

$$S_0 = \frac{\sin 2\theta_m}{2\theta_m}. \qquad (3)$$

The isotropic case $S_0 = 0$ corresponds to $\theta_m = \pi/2$. The smaller the value of θ_m is the higher the order parameter, S_0. We believe that applied simplified distribution function should not affect qualitatively the main results as compared with that for more complicated distribution functions (e.g., normal, wrapped normal, exponential, or von Mises [23]). During the deposition of particles according to the RSA protocol, some particle orientations may be rejected, therefore the actual order parameter in the deposit, S, may differ from the value of S_0. This situation resembles the RSA deposition of partially oriented elongated particles (k-mers) onto a square lattice [60]. The actual order parameter S is conserved only for isotropic ($S_0 = 0$) and completely aligned ($S_0 = 1$) packing, while in the general case, the value of S depends upon the packing fraction, φ. Figure 2 presents examples of the actual order parameter, S, versus the packing fraction, φ, for the preassigned order parameters $S_0 = 0.5$ and $S_0 = 0.9$ and different aspect ratios ε. Here the values of φ_j correspond to jamming states. When the aspect ratio is large, the difference between S and S_0 may be fairly significant. For elongated particles, the actual values of S exceeded the preassigned ones S_0. This possibly reflected formation of domain structures with near-parallel particles inside them. However, for intermediate value $S_0 = 0.5$ and small aspect ratio $\varepsilon = 2$ (Fig. 2), the surprising decreasing of the actual order parameter near the jamming limit φ_j was observed. We have no explanation for
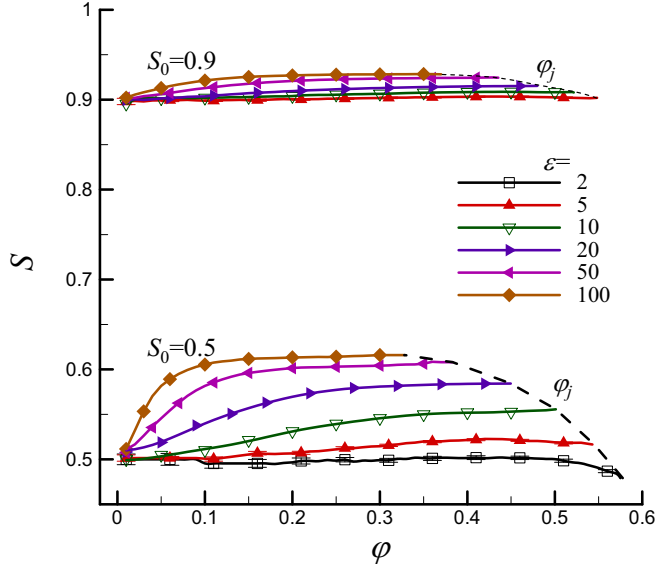
FIG. 2. Actual order parameter, S, versus the packing fraction, φ, at different values of the aspect ratio ε. Examples for the preassigned order parameters $S_0 = 0.5$ and $S_0 = 0.9$. The values of φ_j correspond to jamming states.
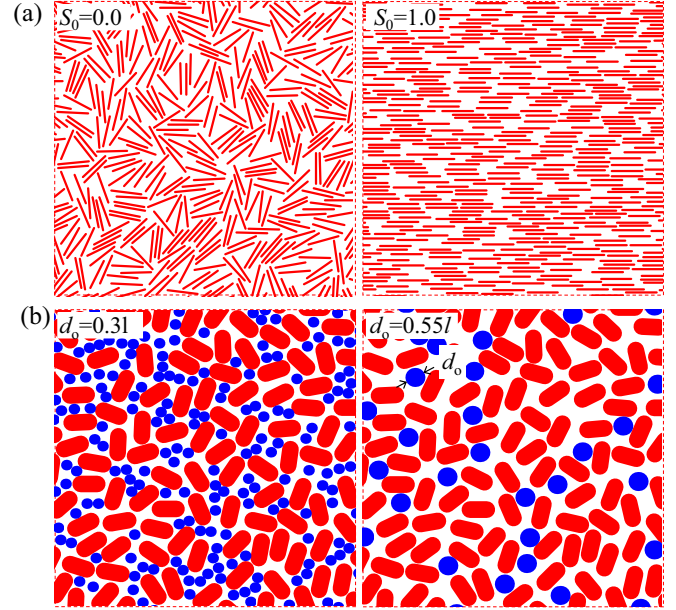

FIG. 3. Examples of the jamming patterns for aspect ratio $\varepsilon = 10$ at $S_0 = 0$ (random orientation) and $S_0 = 1$ (complete alignment along the horizontal direction) (a), and for aspect ratio $\varepsilon = 2$ at $S_0 = 0$ (b). For the latter case, the void space between the discorectangles is filled with reference disks with diameters $d_\circ = 0.3l$ and $d_\circ = 0.55l$. Fragments with size of $9l \times 9l$ are shown.

this behavior; however, note that it is strikingly similar to the cusplike anomaly of jamming coverage for slightly elongated particles. In a similar manner, this orientation effect can reflect the competition between the tendency for maximum packing and excluded volume effects.

The dimensions of the system under consideration were L along both the horizontal (x) and the vertical (y) axes. In the present work, all calculations have been performed using $L = 32l$. The jamming coverage was assumed to be reached after at least $L^2 \times 10^{10}$ unsuccessful attempts to place a new particle on the line. For each given value of ε and S_0, the computer experiments were repeated up to 100 times. The error bars in the figures correspond to the standard deviation of the mean. When not shown explicitly, they are of the order of the marker size. All simulations were performed for the aspect ratios $\varepsilon \in [1; 100]$.

In the resulting deposits, the particles cannot touch each other, hence, they are not in direct contact. However, a core-shell model of the particles can be used to evaluate the connectedness of the particles. To perform this analysis, each particle was covered by an outer shell with a thickness δ (Fig. 1). Any two particles are assumed to be connected when the minimal distance between their hard cores does not exceed the value of 2δ.

The minimum (critical) value of the outer shell thickness δ required for the formation of spanning clusters along the x or y direction, was evaluated. The calculations were performed using the Hoshen-Kopelman algorithm [61]. The analysis was carried out using a list of near-neighbor particles [62].

Figure 3(a) presents examples of the jamming patterns for a fixed aspect ratio of $\varepsilon = 10$ at $S_0 = 0$ (random orientation) and $S_0 = 1$ (complete alignment along the horizontal direction x). An analysis of the holes between discorectangles was undertaken using reference disks of different diameters, $d_\circ$. In these tests, after the formation of the jamming deposits,

the "accessible void" was supplementarily filled with the reference disks using the RSA model up to the jamming limit. Figure 3(b) presents examples of the jamming patterns for the aspect ratio $\varepsilon = 2$ and random orientation of the discorectangles ($S_0 = 0$) for $d_\circ = 0.3l$ and $d_\circ = 0.55l$.

III. RESULTS AND DISCUSSION

Figure 4(a) presents the packing fraction, φ, versus the deposition time, t, for the disordered RSA packing ($S_0 = 0$) of discorectangles with different aspect ratios ε. The value of φ gradually increased with increasing t as the system approached the jamming value φ_j at $t \to \infty$. Similar dependencies $\varphi(t)$ were also observed for other values of S_0. The inflections in the time derivatives $d\varphi/d\log_{10} t$ were used to estimate the characteristic deposition times, τ [Fig. 4(b)] [63].

Figure 5(a) shows the packing fraction at the jamming state, φ_j, versus the discorectangle aspect ratio, ε, at different values of the preassigned order parameter, S_0. For partially disordered systems (at $S_0 < 1$) noticeable cusps (maximums) in the $\varphi_j(\varepsilon)$ dependencies could be observed. For example, for completely disordered RSA packing ($S_0 = 0$) a well-defined maximum $\varphi_j = 0.583 \pm 0.004$ (at $\varepsilon \approx 1.46$) was observed, and this result is in good correspondence with a previously reported value for completely disordered discorectangles, $\varphi_j = 0.582896 \pm 0.000019$ [36]. The initial density increase can be explained by relaxing the parameter constraint (appearance of orientational degrees of freedom) in the RSA packing of the elongated particles, while the density decrease at larger values of ε may reflect excluded volume effects [43]. An increase of partial ordering noticeably influenced the character of the $\varphi_j(\varepsilon)$ dependencies, and the cusps became less significant.
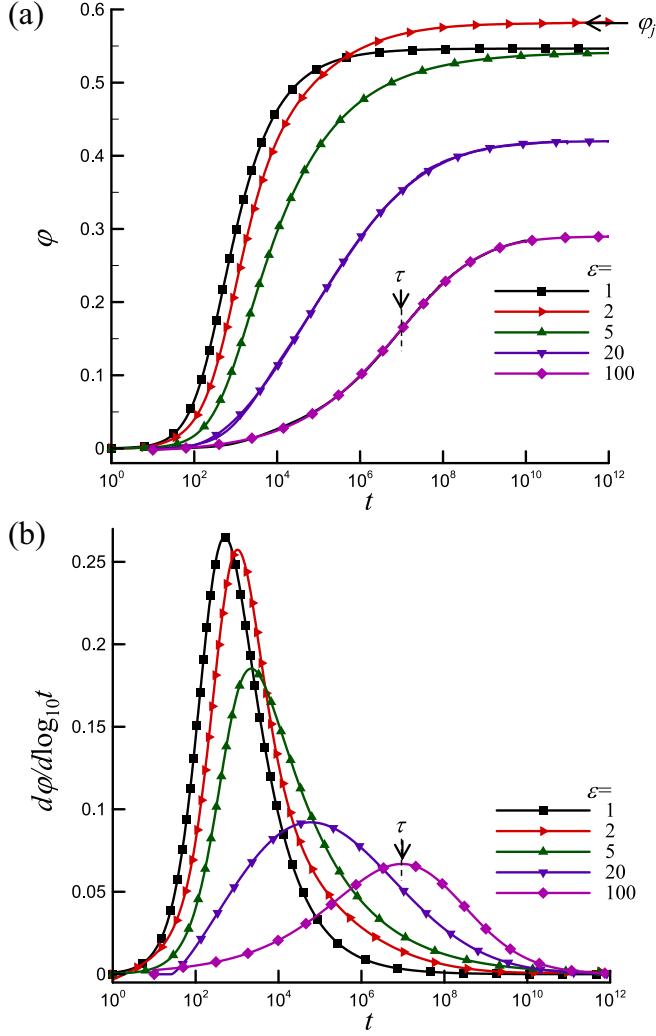
FIG. 4. Packing fraction, φ, (a) and time derivative $d\varphi/d\log_{10} t$ (b) versus the deposition time, t, for the disordered RSA packing ($S_0 = 0$) of discorectangles with aspect ratio ε. Here φ_j is the jamming coverage and τ is the characteristic deposition time.

FIG. 5. Packing fraction at the jamming state, φ_j, (a) and characteristic deposition time, τ, (b) versus the discorectangle aspect ratio, ε, at different values of the preassigned order parameter, S_0.

A remarkable feature was the presence of a stable point at $\varepsilon \simeq 4$ with nearly the same values of $\varphi_j = 0.557 \pm 0.002$ for all values of $S_0 \in [0; 1]$. In the limit of completely aligned discorectangles ($S_0 \to 1$) the cusp disappeared. For this case, the packing fraction gradually increased with ε and approached the value $\varphi_j \approx C_R^2 = 0.5589\ldots$ [Fig. 5(a)], where C_R is the well-known Rényi's parking constant for a 1D problem [64]. This supports Palásti's conjecture, regarding the relationships of the jamming limits for 1D and 2D problems [65].

Figure 5(b) shows the characteristic deposition time, τ, versus the discorectangle aspect ratio, ε, at different values of the preassigned order parameter, S_0. At relatively small aspect ratios ($\varepsilon \leqslant 10$) an approximately linear increase of τ with ε for all values of S_0 was observed:

$$\tau = \tau_1 + a(\varepsilon - 1), \tag{4}$$

where $\tau_1 = 490 \pm 12$ corresponds to the characteristic deposition time for disks ($\varepsilon = 1$) and $a = 508 \pm 6$ (the coefficient of determination was $R^2 = 0.9987$).
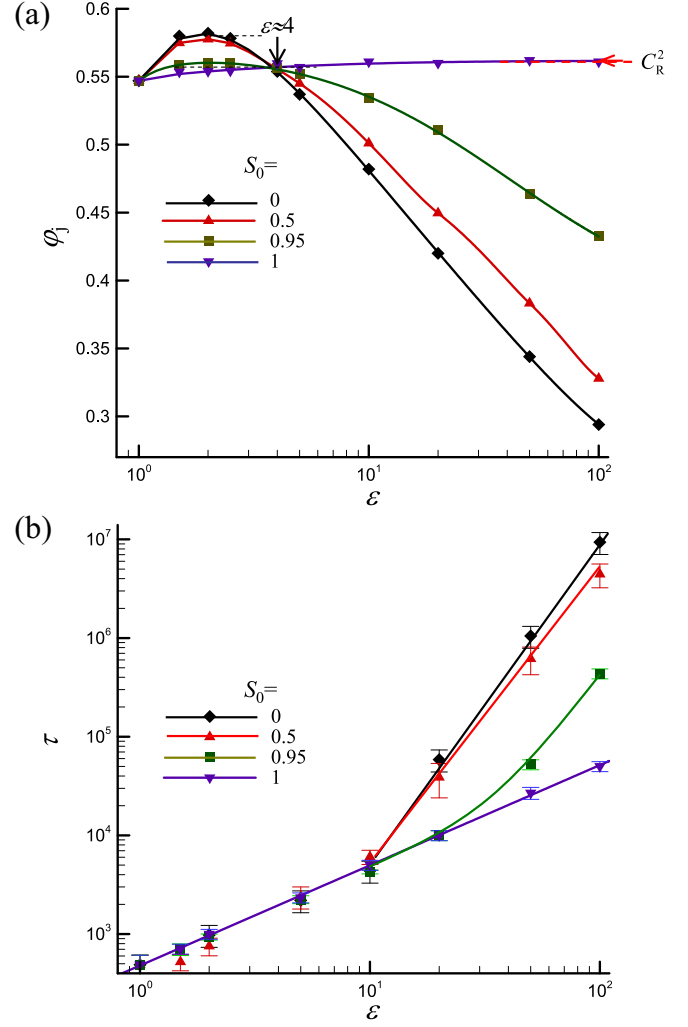
For completely aligned systems ($S_0 = 1$), this linear $\tau(\varepsilon)$ dependence was also observed for $\varepsilon > 10$. For partially oriented systems ($S_0 < 1$), significant deviations were observed for $\varepsilon > 10$, particularly for $S_0 = 0$. This reflected the excluded volume effects on stagnation of the RSA deposition process for disordered systems. For these systems, the packing fraction at the jamming state, φ_j significantly decreased for elongated particles with large aspect ratio ε. This also reflected the excluded volume effects on packing loosening [23].

The evaluated characteristic time can reflect the transition from initial loose uncorrelated packing to the more dense correlated packing at longer time. Moreover, for relatively long particles ($\varepsilon > 10$), the value of τ may reflect stagnated deposition of particles inside domains of previously deposited particles. For this case, the voids in domains can be filled only with the particles with some specific orientations, and the adsorption rate is slowing down.

Figure 6 demonstrates examples of the minimal reduced thickness of the shell, δ/d, required for a spanning path through the system, versus the packing fraction, φ, at a fixed preassigned order parameter $S_0 = 0.0$ and different aspect
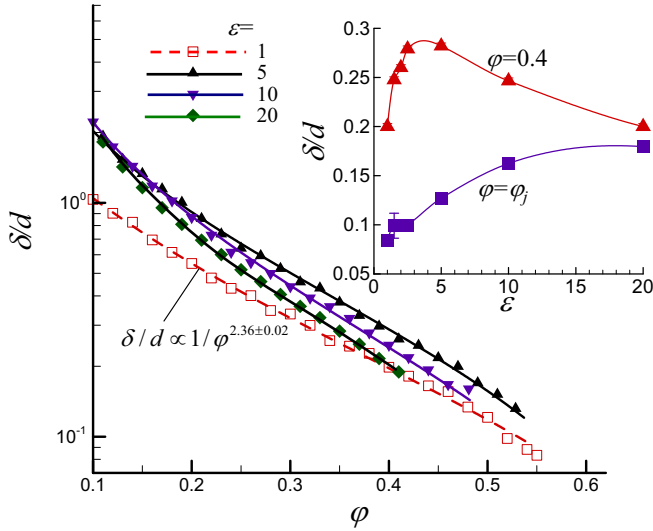
FIG. 6. Minimal reduced thickness of shell, δ/d, required for infinite connectivity between particles (formation of a spanning path through the system), versus the packing fraction, φ, at different aspect ratios ε. The preassigned order parameter is $S_0 = 0.0$. The inset shows the δ/d versus ε dependencies at $\varphi = 0.4$ and $\varphi = \varphi_j$ (jamming state).
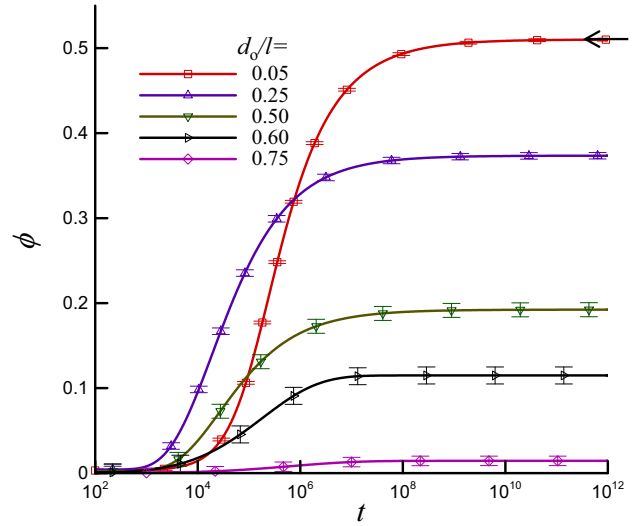

FIG. 7. Packing fraction of reference disks, ϕ, versus the deposition time, t. Here discorectangles with an aspect ratio of $\varepsilon = 2$ and random orientations ($S_0 = 0$) were preliminarily deposited to the jamming state ($\varphi_j \approx 0.582$), and then RSA packing of reference disks with different diameters $d_\circ$ into the confined void spaces between the discorectangles was applied. The value ϕ_j corresponds to the jamming coverage of the reference disks.

ratios ε. The values of δ/d decreased with φ, particularly, the power relation $\delta/d \propto 1/\varphi^\alpha$ ($\alpha = 2.36 \pm 0.02$) could be observed at $\varepsilon = 1$. However, the connectivity behavior at different values of ε was rather complex (see inset in Fig. 6). For example, at a fixed value of $\varphi = 0.4$, the connectivity analysis revealed a cusp (maximum) in the $\delta(\varepsilon)/d$ dependence. This maximum is similar to that observed in the $\varphi_j(\varepsilon)$ dependence and it evidently reflects the interplay of the above-mentioned geometrical effects (orientation freedom and excluded volume). For the maximum packing (jamming state) the value of δ/d increased with ε, i.e., the connectivity did not display any cusp behavior (see inset in Fig. 6).

Figure 7 demonstrates examples of the packing fraction of reference disks, ϕ, versus the deposition time, t. The value of ϕ was calculated as the total area of disks divided by the area not covered by discorectangles. In these simulations, discorectangles with an aspect ratio of $\varepsilon = 2$ and random orientations ($S_0 = 0$) were preliminarily deposited to the jamming state ($\varphi_j \approx 0.582$). Then RSA packing of reference disks with different diameters $d_\circ$ into the confined void spaces between the discorectangles was applied. The value ϕ_j corresponds to the jamming coverage of the reference disks, and with small disks ($d_0/l \ll 1$), it was close to the value of $\phi_j \approx 0.547$ for the jamming coverage of disks seen for an nonconfined RSA problem on a plane [29,30].

Figure 8 compares the ϕ_j versus $d_\circ/l$ dependencies for completely disordered ($S_0 = 0$, filled symbols, solid lines) and completely aligned ($S_0 = 1$, open symbols, dashed lines) discorectangles at different aspect ratios, ε. The values of ϕ_j gradually decreased with $d_\circ/l$ and where RSA packing was possible for reference disks with sizes not exceeding some maximum size d_m/l. The character of the $\phi_j(d_\circ/l)$ dependencies were noticeably different for different values of ε. They were approximately linear at some intermediate

values of the aspect ratio $\varepsilon \approx 2$, demonstrated convexity when $\varepsilon < 2$, and concavity when $\varepsilon > 2$. Moreover, the value of ε differently affected the maximum diameter d_m/l in the dependence on S_0 (see inset in Fig. 7). At small values of ε ($\varepsilon \lesssim 4$) the value of d_m/l for a completely aligned system ($S_0 = 1$) exceeded that for a completely disordered system
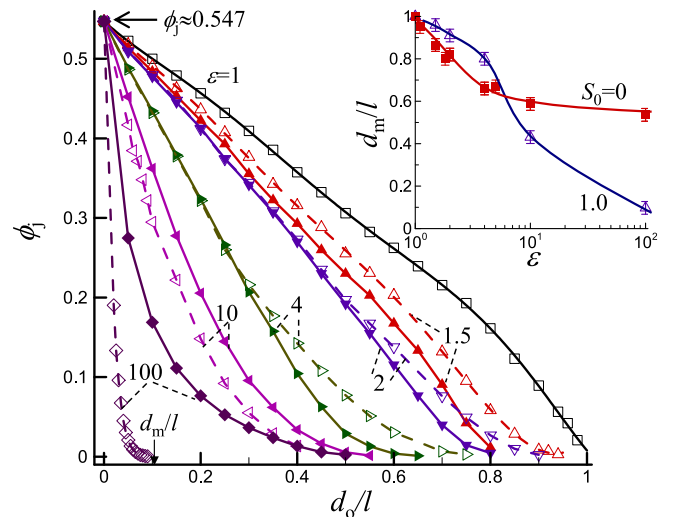

FIG. 8. Jamming packing fraction of reference disks in the void space between discorectangles, ϕ_j, versus reduced diameter of the disks $d_\circ/l$. The data are presented for completely disordered ($S_0 = 0$, filled symbols, solid lines) and completely aligned ($S_0 = 1$, open symbols, dashed lines) discorectangles with different aspect ratios of ε. The value of d_m/l corresponds to the maximum diameter of the reference disks. Inset shows the d_m/l versus ε dependencies for different values of the preassigned order parameters, S_0.

($S_0 = 0$), but the situation was inverse at large values of ε ($\varepsilon > 4$). For large aspect ratios ($\varepsilon \gg 1$) a different limiting behavior was also observed, $d_{\mathrm{m}}/l \to 0.5$ for $S_0 = 0$ and $d_{\mathrm{m}}/l \to 0$ for $S_0 = 1$. For relatively large values of ε the relatively large holes ("empty" spaces) between the discorectangles can be distinguished accounting for the side-to-side, side-to-cap, and cap-to-cap positions of the near-neighbor discorectangles (Fig. 3). This distinction is governed by the preassigned order parameter, S_0, and a decreased value of this results in an increase in the size of the holes (value of d_{m}/l). Note that side-to-side contacts were expected to play a stabilizing role in the packing of elongated particles [66].

IV. CONCLUSION

Simulations for a continuous 2D model of RSA packing of discorectangles have been performed. The initial state was produced at different values of the preassigned order parameters $0 \leqslant S_0 \leqslant 1$. The effects of ordering on the packings were noticeably dependent on the discorectangle aspect ratio, ε. For partially disordered systems ($S_0 < 1$) and at relatively small values of ε ($\varepsilon < 4$), the dependencies of the jamming coverage $\varphi_{\mathrm{j}}(\varepsilon)$ showed that the cusps. For more elongated particles ($\varepsilon > 4$), the values of φ_{j} decreased with ε. However, for completely aligned discorectangles ($S_0 = 1$) the cusps dis-

appeared, and the value of φ_{j} gradually increased with ε and approached the value $\varphi_{\mathrm{j}} \approx C_{\mathrm{R}}^2$, where C_{R} is the Rényi's parking constant for a 1D problem [64]. Therefore, Palásti's conjecture, that jamming coverages in 1D and 2D are connected as $\varphi_{\mathrm{j,2D}} = \varphi_{\mathrm{j,1D}}^2$, is fulfilled [65]. At $\varepsilon = 4$, we observed almost the same value of $\varphi_{\mathrm{j}} = 0.557 \pm 0.002$ for all values of $S_0 \in [0; 1]$. The complex effects of aspect ratio and orientation ordering on the connectivity of discorectangles with coreshell structures and on the distribution of local voids between discorectangles were also revealed.

Note that the previous studies performed in equilibrium state for rod with large aspect ratio ($\varepsilon \gg 1$) revealed conditions for the transition from RSA to the quasinematic phase [50]. Therefore, it might be very interesting in future to investigate the relaxation of irreversible RSA packing of discorectangles with finite aspect ratios towards the equilibrium state.

[1] T. Börzsönyi and R. Stannarius, Granular materials composed of shape-anisotropic grains, Soft Matter **9**, 7401 (2013).

[2] J. Gan and A. Yu, DEM study on the packing density and randomness for packing of ellipsoids, Powder Technol. **361**, 424 (2020).

[3] J. Gan and A. Yu, DEM simulation of the packing of cylindrical particles, Granul. Matter **22**, 22 (2020).

[4] L. Onsager, The effects of shape on the interaction of colloidal particles, Ann. N.Y. Acad. Sci. **51**, 627 (1949).

[5] P. Bolhuis and D. Frenkel, Tracing the phase boundaries of hard spherocylinders, J. Chem. Phys. **106**, 666 (1997).

[6] T. Marschall, Y.-E. Keta, P. Olsson, and S. Teitel, Orientational Ordering in Athermally Sheared, Aspherical, Frictionless Particles, Phys. Rev. Lett. **122**, 188002 (2019).

[7] A. B. Yu, X. Z. An, R. P. Zou, R. Y. Yang, and K. Kendall, Self-Assembly of Particles for Densest Packing by Mechanical Vibration, Phys. Rev. Lett. **97**, 265501 (2006).

[8] Q. Qian, X. An, H. Zhao, K. Dong, Y. Wu, H. Fu, H. Zhang, and X. Yang, Particle scale study on the crystallization of mono-sized cylindrical particles subject to vibration, Powder Technol. **352**, 470 (2019).

[9] R. P. Zou and A. B. Yu, Evaluation of the packing characteristics of mono-sized non-spherical particles, Powder Technol. **88**, 71 (1996).

[10] R. Guises, J. Xiang, J.-P. Latham, and A. Munjiza, Granular packing: Numerical simulation and the characterisation of the effect of particle shape, Granul. Matter **11**, 281 (2009).

[11] A. V. Kyrylyuk and A. P. Philipse, Effect of particle shape on the random packing density of amorphous solids, Phys. Status Solidi A **208**, 2299 (2011).

[12] A. K. H. Kwan and C. F. Mora, Effects of various shape parameters on packing of aggregate particles, Mag. Concr. Res. **53**, 91 (2001).

[13] C. R. A. Abreu, F. W. Tavares, and M. Castier, Influence of particle shape on the packing and on the segregation of spherocylinders via Monte Carlo simulations, Powder Technol. **134**, 167 (2003).

[14] E. Azéma and F. Radjaï, Force chains and contact network topology in sheared packings of elongated particles, Phys. Rev. E **85**, 031303 (2012).

[15] V. Chen and M. Hlavacek, Application of Voronoi tessellation for modeling randomly packed hollow-fiber bundles, AIChE J. **40**, 606 (1994).

[16] L. Bokobza, Natural rubber nanocomposites: A review, Nanomater. Basel **9**, 12 (2019).

[17] L. Yang, Z. Zhou, J. Song, and X. Chen, Anisotropic nanomaterials for shape-dependent physicochemical and biomedical applications, Chem. Soc. Rev. **48**, 5140 (2019).

[18] N. P. Pampaloni, M. Giugliano, D. Scaini, L. Ballerini, and R. Rauti, Advances in nano neuroscience: From nanomaterials to nanotools, Front. Neurosci. **12**, 953 (2019).

[19] N. Lebovka, L. Lisetski, and L. Bulavin, Organization of nanodisks of laponite® in soft colloidal systems, in *Modern Problems of the Physics of Liquid Systems*, edited by L. A. Bulavin and L. Xu (Springer, Cham, 2019), pp. 137–164.

[20] M. Wang, Y. Liu, B. Qi, A. Al-Tabbaa, and W. Wang, Percolation and conductivity development of the rod networks within randomly packed porous media, Compos. Part B Eng. **187**, 107837 (2020).

[21] J. Hirotani and Y. Ohno, Carbon nanotube thin films for high-performance flexible electronics applications, Top. Curr. Chem. **377**, 3 (2019).

[22] I. Tiginyanu, P. Topala, and V. Ursaki, editors, *Nanostructures and Thin Films for Multifunctional Applications. Technology, Properties and Devices* (Springer Nature, Cham, 2016).

[23] N. I. Lebovka and Y. Y. Tarasevich, Two-dimensional systems of elongated particles: From diluted to dense, in *Order, Disorder and Criticality. Advanced Problems of Phase Transition Theory*, Vol. 6, edited by Y. Holovatch (World Scientific, Singapore, 2020), pp. 153–183.

[24] E. Basurto, P. Gurin, S. Varga, and G. Odriozola, Ordering, clustering, and wetting of hard rods in extreme confinement, Phys. Rev. Res. **2**, 013356 (2020).

[25] D. Frenkel and R. Eppenga, Evidence for algebraic orientational order in a two-dimensional hard-core nematic, Phys. Rev. A **31**, 1776 (1985).

[26] M. A. Bates and D. Frenkel, Phase behavior of two-dimensional hard rod fluids, J. Chem. Phys. **112**, 10034 (2000).

[27] J. W. Evans, Random and cooperative sequential adsorption, Rev. Mod. Phys. **65**, 1281 (1993).

[28] R. Miskin, Nonlinear transport of particles, in *Particles at Interfaces, Interface Science and Technology*, Vol. 20, edited by Z. Adamczyk (Elsevier, Amsterdam, 2017), pp. 513–679.

[29] L. Finegold and J. T. Donnell, Maximum density of random placing of membrane particles, Nature (London) **278**, 443 (1979).

[30] J. Feder, Random sequential adsorption, J. Theor. Biol. **87**, 237 (1980).

[31] J. D. Sherwood, Random sequential adsorption of lines and ellipses, J. Phys. A: Math. Gen. **23**, 2827 (1990).

[32] P. Viot and G. Tarjus, Random sequential addition of unoriented squares: Breakdown of Swendsen's conjecture, Europhys. Lett. **13**, 295 (1990).

[33] R. D. Vigil and R. M. Ziff, Random sequential adsorption of unoriented rectangles onto a plane, J. Chem. Phys. **91**, 2599 (1989).

[34] R. D. Vigil and R. M. Ziff, Kinetics of random sequential adsorption of rectangles and line segments, J. Chem. Phys. **93**, 8270 (1990).

[35] S. M. Ricci, J. Talbot, G. Tarjus, and P. Viot, A structural comparison of random sequential adsorption and equilibrium configurations of spherocylinders, J. Chem. Phys. **101**, 9164 (1994).

[36] K. Haiduk, P. Kubala, and M. Cieśla, Saturated packings of convex anisotropic objects under random sequential adsorption protocol, Phys. Rev. E **98**, 063309 (2018).

[37] M. Cieśla and J. Barbasz, Random packing of regular polygons and star polygons on a flat two-dimensional surface, Phys. Rev. E **90**, 022402 (2014).

[38] G. Zhang, Precise algorithm to generate random sequential adsorption of hard polygons at saturation, Phys. Rev. E **97**, 043311 (2018).

[39] M. Cieśla and J. Barbasz, Modelling of interacting dimer adsorption, Surf. Sci. **612**, 24 (2013).

[40] M. Cieśla, Continuum random sequential adsorption of polymer on a flat and homogeneous surface, Phys. Rev. E **87**, 052401 (2013).

[41] M. Cieśla, G. Pająk, and R. M. Ziff, Shapes for maximal coverage for two-dimensional random sequential adsorption, Phys. Chem. Chem. Phys. **17**, 24376 (2015).

[42] P. Viot, G. Tarjus, S. M. Ricci, and J. Talbot, Random sequential adsorption of anisotropic particles. I. Jamming limit and asymptotic behavior, J. Chem. Phys. **97**, 5212 (1992).

[43] P. M. Chaikin, A. Donev, W. Man, F. H. Stillinger, and S. Torquato, Some observations on the random packing of hard ellipsoids, Ind. Eng. Chem. Res. **45**, 6960 (2006).

[44] A. Baule, Shape Universality Classes in the Random Sequential Adsorption of Nonspherical Particles, Phys. Rev. Lett. **119**, 028003 (2017).

[45] M. Cieśla, K. Kozubek, P. Kubala, and A. Baule, Kinetics of random sequential adsorption of two-dimensional shapes on a one-dimensional line, Phys. Rev. E **101**, 042901 (2020).

[46] N. I. Lebovka, M. O. Tatochenko, N. V. Vygornitskii, and Y. Y. Tarasevich, Paris car parking problem for partially oriented discorectangles on a line, Phys. Rev. E **102**, 012128 (2020).

[47] J. Talbot, G. Tarjus, and P. Schaaf, Unexpected asymptotic behavior in random sequential adsorption of nonspherical particles, Phys. Rev. A **40**, 4808 (1989).

[48] B. J. Brosilow, R. M. Ziff, and R. D. Vigil, Random sequential adsorption of parallel squares, Phys. Rev. A **43**, 631 (1991).

[49] O. Gromenko and V. Privman, Random sequential adsorption of oriented superdisks, Phys. Rev. E **79**, 042103 (2009).

[50] N. I. Lebovka, N. V. Vygornitskii, and Y. Y. Tarasevich, Relaxation in two-dimensional suspensions of rods as driven by Brownian diffusion, Phys. Rev. E **100**, 042139 (2019).

[51] T. Ackermann, R. Neuhaus, and S. Roth, The effect of rod orientation on electrical anisotropy in silver nanowire networks for ultra-transparent electrodes, Sci. Rep. **6**, 34289 (2016).

[52] Y. Wu, Z. Jiang, X. Zan, Y. Lin, and Q. Wang, Shear flow induced long-range ordering of rod-like viral nanoparticles within hydrogel, Colloids Surf., B **158**, 620 (2017).

[53] J. Shaver, A. N. G. Parra-Vasquez, S. Hansel, O. Portugall, C. H. Mielke, M. von Ortenberg, R. H. Hauge, M. Pasquali, and J. Kono, Alignment dynamics of single-walled carbon nanotubes in pulsed ultrahigh magnetic fields, ACS Nano **3**, 131 (2009).

[54] M. Mohammadimasoudi, Z. Hens, and K. Neyts, Full alignment of dispersed colloidal nanorods by alternating electric fields, RSC Adv. **6**, 55736 (2016).

[55] B. M. I. van der Zande, G. J. M. Koper, and H. N. W. Lekkerkerker, Alignment of rod-shaped gold particles by electric fields, J. Phys. Chem. B **103**, 5754 (1999).

[56] C. Vega and S. Lago, A fast algorithm to evaluate the shortest distance between rods, Comput. Chem. **18**, 55 (1994).

[57] L. Pournin, M. Weber, M. Tsukahara, J.-A. Ferrez, M. Ramaioli, and T. M. Liebling, Three-dimensional distinct element simulation of spherocylinder crystallization, Granul. Matter **7**, 119 (2005).

[58] V. V. Mahajan, T. M. J. Nijssen, J. A. M. Kuipers, and J. T. Padding, Non-spherical particles in a pseudo-2D fluidised bed: Modelling study, Chem. Eng. Sci. **192**, 1105 (2018).

[59] I. Balberg and N. Binenbaum, Computer study of the percolation threshold in a two-dimensional anisotropic system of conducting sticks, Phys. Rev. B **28**, 3799 (1983).

[60] N. I. Lebovka, N. N. Karmazina, Y. Y. Tarasevich, and V. V. Laptev, Random sequential adsorption of partially oriented linear *k*-mers on a square lattice, Phys. Rev. E **84**, 061603 (2011).

[61] J. Hoshen and R. Kopelman, Percolation and cluster distribution. I. Cluster multiple labeling technique and critical concentration algorithm, Phys. Rev. B **14**, 3438 (1976).

[62] S. C. van der Marck, Percolation thresholds and universal formulas, Phys. Rev. E **55**, 1514 (1997).

[63] R. C. Hart and F. D. A. Aarão Reis, Random sequential adsorption of polydisperse mixtures on lattices, Phys. Rev. E **94**, 022802 (2016).

[64] A. Rényi, On a one-dimensional problem concerning random space filling, Sel. Transl. Math. Stat. Probab. **4**, 203 (1963), translation from Magyar Tud. Akad. Mat. Kutató Int. Közl. 3, No. 1–2, 109 (1958).

[65] I. Palásti, On some random space filling problems, Magyar Tud. Akad. Mat. Kutató Int. Közl. **5**, 353 (1960).

[66] E. Azéma and F. Radjaï, Stress-strain behavior and geometrical properties of packings of elongated particles, Phys. Rev. E **81**, 051304 (2010).